Proximity-induced superconductivity in monolayer CuO_2 on cuprate substrates

Guo-Yi Zhu,[1] Fu-Chun Zhang,[2,3] and Guang-Ming Zhang[1,4]

[1]*State Key Laboratory of Low-Dimensional Quantum Physics and Department of Physics, Tsinghua University, Beijing 100084, China*

[2]*Department of Physics, Zhejing University, Hangzhou 310027, China*

[3]*Collaborative Innovation Center of Advanced Microstructures, Nanjing 210093, China*

[4]*Collaborative Innovation Center of Quantum Matter, Beijing 100084, China*

(Received 18 August 2016; revised manuscript received 17 October 2016; published 3 November 2016)

To understand the recently observed high temperature superconductivity in the monolayer CuO_2 grown on the $Bi_2Sr_2CaCu_2O_{8+\delta}$ substrates, we propose a two-band model of the hybridized oxygen p_x and p_y orbitals with the proximity effect of the substrate. We demonstrate that both the nodal and nodeless superconducting states can be induced by the proximity effect, depending on the strengths of the pairing parameters.

DOI: 10.1103/PhysRevB.94.174501

I. INTRODUCTION

High transition temperature (T_c) superconductivity in cuprates remains one of the most challenging topics in condensed matter physics [1–4]. Despite world-wide efforts in the past 30 years, the physics community has still not reached a consensus on what causes T_c to be so high. All the high T_c superconducting copper oxides have layered structures; the superconducting layers CuO_2 are sandwiched by nonconducting charge reservoir layers. Modulation of charge carriers in the CuO_2 planes is realized through substitution of chemical elements in nonconducting planes, a key parameter in the study of the high T_c superconductors.

Recently, Zhong *et al.* reported that a monolayer CuO_2 is successfully grown on $Bi_2Sr_2CaCu_2O_{8+\delta}$ (Bi-2212) substrates via molecular beam epitaxy (MBE) [5]. Their result is interesting and important [6]. Unlike the sandwiched CuO_2 layers in the bulk Bi-2212, a monolayer CuO_2 is on the BiO surface of the top substrates, which opens a route for most direct probes such as scanning tunneling microscopy (STM) on the high T_c copper oxides. Two distinct and spatially separated energy gaps are observed on the films: the V-shaped gap is similar to the gap observed on the BiO layer, and the U-shaped gap is of superconducting nature and is nodeless. The latter is also immune to scattering by K, Cs, and Ag atoms. The observed U-like gap is in striking contrast with the nodal gap in the $d_{x^2-y^2}$-wave pairing symmetry which is well established in the bulk cuprates [7–9]. The reported superconductivity in the monolayer CuO_2 raises two important questions. One is the nature of its superconductivity: Is it the same as the superconductivity of the Bi-2212 substrates or a new superconducting state? The other is its pairing symmetry.

We begin with a brief summary of the electronic structure of the high T_c superconducting copper oxides. The parent compounds of the copper oxides are antiferromagnetic Mott insulators, and superconductivity arises upon chemical doping, which introduces charge carriers in the CuO_2 planes. The layers in cuprates are generally charged, either with positive charge such as in the BiO layer in Bi-2212 or with negative charge such as in the sandwiched CuO_2 layer. The charge carriers on the CuO_2 plane in the parent compound is $-2e$ per unit cell consisting of one copper and two oxygen atoms. The copper has a valence of $2+$ and is in $3d^9$ configuration with a single hole of $d_{x^2-y^2}$ orbital, and oxygen has a valence of $2-$ and is in configuration of $2p^6$. Due to the strong on-site Coulomb repulsion, each Cu atom is occupied with a single $3d$ hole carrying spin-1/2 moment. Chemical doping introduces additional holes into the CuO_2 plane. These additional holes primarily reside on the oxygen sites, forming the Zhang-Rice spin singlets, which move through the square lattice of Cu ions by exchanging with neighboring Cu spin-1/2 moment. This leads to an effective two-dimensional t-J model or large on-site repulsive Hubbard model [10]. This model describes some of the elementary low-temperature physics in hole doped cuprates. In the relevant parameter region, the carrier density introduced by doping is typically $0.1 \sim 0.25$ hole per unit cell in bulk superconducting cuprates.

We now turn to examine the electronic structure of the MBE grown monolayer CuO_2 on the top of a BiO layer, which is the surface plane of the charge neutral Bi-2212 substrate. If we neglect the charge transfer from the monolayer CuO_2 to the inner planes, the monolayer CuO_2 is charge neutral as required by total charge neutrality. Therefore, the Cu ion has a valence of $2+$, or $3d^9$ configuration, while the oxygen ion has a valence of $1-$ and is hence in configuration of $2p^5$ in the monolayer CuO_2. The charge carriers in the CuO_2 monolayer thus have an additional two holes in average on the oxygen ions per unit cell, which is in contrast with the bulk superconducting cuprates. It is expected that some charge carriers on the monolayer CuO_2 may be transferred to the inner planes of the substrate Bi-2212, so that the actual charge carriers on the oxygen ions will be slightly reduced. With such a large charge carrier concentration, we expect the CuO_2 monolayer itself to be a good metal, whose low energy physics is totally different from the cuprates near a Mott insulator.

In this paper we propose that the superconductivity observed in the CuO_2 monolayer is proximity-induced superconductivity from the substrate cuprate. The primary reason in support of this scenario is that the transition temperature of the superconductivity in the monolayer is essentially the same as that of the Bi-2212 substrates as reported in Ref. [5]. The challenge to this scenario is to explain the U-shaped superconducting gap in the monolayer. We shall examine a two-band model for the monolayer, which is coupled to the d-wave superconducting substrate by proximity effect. We show that in a certain parameter region, a two-band d-wave proximity-induced superconductivity may be gapful with a U-shaped gap. We expect the monolayer to exhibit a lower T_c

if the substrate has a lower T_c or nonsuperconducting if the substrate is nonsuperconducting. So the present theory can be tested and distinguished in experiments.

The rest of the paper is organized as follows. In the next section, we present a model Hamiltonian for proximity-induced superconductivity in monolayer CuO_2. In the third section, we discuss the possible nodeless superconducting gap of the model and present numerical results for the phase diagram on the nodal or nodeless superconducting phases. The paper ends with a short summary and discussion.

II. TWO-BAND MODEL FOR MONOLAYER CuO_2 AND ITS PROXIMITY EFFECT INDUCED d-WAVE SUPERCONDUCTIVITY

In this section, we propose a two-band model for the monolayer CuO_2 on the Bi-2212 substrate and examine the proximity effect induced d-wave superconductivity. We first discuss the Hamiltonian part without the pairing, i.e., a noninteracting electron system on a square lattice with oxygen orbitals of either $2p_x$ or $2p_y$ as shown in Fig. 1, whose Hamiltonian is given by

$$H_0 = \sum_{\mathbf{k}\sigma} \begin{pmatrix} c^\dagger_{1,\mathbf{k}\sigma} & c^\dagger_{2,\mathbf{k}\sigma} \end{pmatrix} \begin{pmatrix} \epsilon_x & \epsilon_{xy} \\ \epsilon_{xy} & \epsilon_y \end{pmatrix} \begin{pmatrix} c_{1,\mathbf{k}\sigma} \\ c_{2,\mathbf{k}\sigma} \end{pmatrix}, \tag{1}$$

where

$$\begin{aligned} \epsilon_x &= -2(t_x \cos k_x + t_y \cos k_y) - \mu, \\ \epsilon_y &= -2(t_y \cos k_x + t_x \cos k_y) - \mu, \\ \epsilon_{xy} &= -4t_{xy} \cos\frac{k_x}{2} \cos\frac{k_y}{2}, \end{aligned} \tag{2}$$

and t_x, t_y, and t_{xy} are assumed to be positive parameters, and characterize the nearest neighbor intra- and interorbital hopping terms, respectively. A more accurate description for the monolayer would also include the Cu-3$d_{x^2-y^2}$ orbital. The holes on the O site ($2p_x$ and $2p_y$) are strongly coupled to the localized Cu-3$d_{x^2-y^2}$ spin, and the system may be described by the Anderson lattice model with two conduction bands. Roughly speaking, the holes on the Cu site lead to renormalization of the two conduction bands of O orbitals as in the usual Anderson lattice problem. From this point of view, the noninteracting two-band model described in Eq. (1) is a simplified model for the monolayer with the understanding that the conduction bands are renormalized ones.

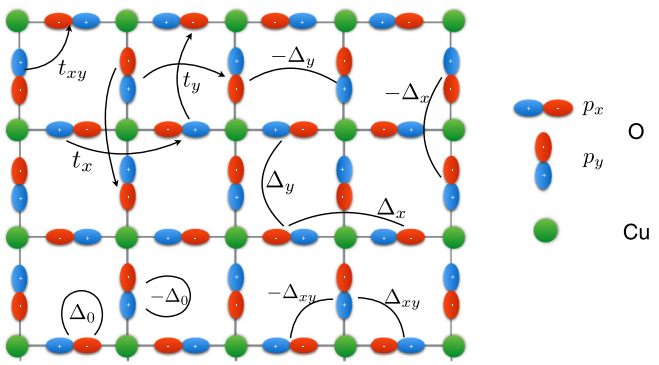

FIG. 1. The monolayer CuO_2 on the cuprate Bi-2212 substrate and our effective two-band model with all possible d-wave proximity pairings.

The interorbital hopping term hybridizes the two orbitals into two bands with dispersion

$$\epsilon_\pm(\mathbf{k}) = \frac{\epsilon_x + \epsilon_y}{2} \pm \sqrt{\left(\frac{\epsilon_x - \epsilon_y}{2}\right)^2 + \epsilon_{xy}^2}. \tag{3}$$

The model is symmetric under reflection with respect to the x axis or y axis (Cu-O bonds) and has C_4 rotational symmetry:

$$\begin{aligned} \epsilon_x(k_x,k_y) &= \epsilon_y(k_y,-k_x), \\ \epsilon_\pm(k_x,k_y) &= \epsilon_\pm(k_y,-k_x). \end{aligned}$$

To describe the proximity effect of the cuprate substrate with d-wave superconductivity, we introduce d-wave pairings for the carriers on the oxygen $2p_x$ and $2p_y$ orbitals as shown in Fig. 1. In the momentum space, the full model Hamiltonian can be written as

$$H = \sum_{\mathbf{k}} \Psi^\dagger_{\mathbf{k}} H(\mathbf{k}) \Psi_{\mathbf{k}}, \tag{4}$$

where the Nambu spinor has been introduced as $\Psi^\dagger_{\mathbf{k}} = (c^\dagger_{1,\mathbf{k}\uparrow} c^\dagger_{2,\mathbf{k}\uparrow} c_{1,-\mathbf{k}\downarrow} c_{2,-\mathbf{k}\downarrow})$, and the Hamiltonian matrix is given by

$$H(\mathbf{k}) = \begin{pmatrix} \epsilon_x & \epsilon_{xy} & \Delta_{xx}(\mathbf{k}) & \Delta_{xy}(\mathbf{k}) \\ \epsilon_{xy} & \epsilon_y & \Delta_{xy}(\mathbf{k}) & \Delta_{yy}(\mathbf{k}) \\ \Delta_{xx}(\mathbf{k}) & \Delta_{xy}(\mathbf{k}) & -\epsilon_x & -\epsilon_{xy} \\ \Delta_{xy}(\mathbf{k}) & \Delta_{yy}(\mathbf{k}) & -\epsilon_{xy} & -\epsilon_y \end{pmatrix}, \tag{5}$$

with

$$\begin{aligned} \Delta_{xx}(\mathbf{k}) &= \Delta_0 + 2(\Delta_x \cos k_x + \Delta_y \cos k_y), \\ \Delta_{yy}(\mathbf{k}) &= -\Delta_0 - 2(\Delta_y \cos k_x + \Delta_x \cos k_y), \\ \Delta_{xy}(\mathbf{k}) &= 4\Delta_{xy} \sin\frac{k_x}{2} \sin\frac{k_y}{2}. \end{aligned} \tag{6}$$

Note that the d-wave pairing symmetry of the substrates requires

$$\Delta_{xx}(\mathbf{k}) = -\Delta_{yy}(\bar{\mathbf{k}}), \quad \Delta_{xy}(\mathbf{k}) = -\Delta_{xy}(\bar{\mathbf{k}}),$$

where $\bar{\mathbf{k}} = (k_y, -k_x)$ and the different pairing components, Δ_0, Δ_x, Δ_y, and Δ_{xy}, are induced by the proximity effect of the d-wave superconducting substrates though their derivation is not included in the present paper [11]. By transforming the gap function matrix for p_x and p_y orbitals into the hybridized band basis, we arrive at

$$\tilde{\Delta}_k(\mathbf{k}) = \begin{pmatrix} \Delta_{++}(\mathbf{k}) & \Delta_{+-}(\mathbf{k}) \\ \Delta_{+-}(\mathbf{k}) & \Delta_{--}(\mathbf{k}) \end{pmatrix}, \tag{7}$$

with

$$\begin{aligned} \Delta_{++}(\mathbf{k}) &= \Delta_d(\mathbf{k}) + \Delta_s(\mathbf{k}) \cos\theta_{\mathbf{k}} - \Delta_{xy}(\mathbf{k}) \sin\theta_{\mathbf{k}}, \\ \Delta_{--}(\mathbf{k}) &= \Delta_d(\mathbf{k}) - \Delta_s(\mathbf{k}) \cos\theta_{\mathbf{k}} + \Delta_{xy}(\mathbf{k}) \sin\theta_{\mathbf{k}}, \\ \Delta_{+-}(\mathbf{k}) &= \Delta_s(\mathbf{k}) \sin\theta_{\mathbf{k}} + \Delta_{xy}(\mathbf{k}) \cos\theta_{\mathbf{k}}, \end{aligned} \tag{8}$$

where $\Delta_s(\mathbf{k}) = \Delta_0 + (\Delta_x + \Delta_y)(\cos k_x + \cos k_y)$, $\Delta_d(\mathbf{k}) = (\Delta_x - \Delta_y)(\cos k_x - \cos k_y)$, and $\theta_{\mathbf{k}} = \tan^{-1}\frac{-2\epsilon_{xy}}{\epsilon_x - \epsilon_y}$ in the range of $[0,\pi]$. It shows that the hybridized bands of p_x and p_y orbitals are subject to the mixture of s-wave and d-wave

pairings, together with $\Delta_{xy}(\mathbf{k})$ which is also d-wave symmetric but nevertheless shows nodal lines along the x or y axis, breaking mirror reflection symmetries with regards to the x or y axis. For consideration of mirror symmetry, we will set $\Delta_{xy} = 0$ in what follows. Actually an analysis of the proximity pairing for the monolayer on top of the substrate Bi-2212 suggests the leading order in Δ_{xy} vanishes [11]. Neglect of this term does not seem to change the qualitative physics we wish to address. Therefore the intraband pairings Δ_{++} and Δ_{--} are dominated by d-wave symmetry with a correction of modulated s-wave component. Under the limit $|\epsilon_{xy}| \gg |\epsilon_x - \epsilon_y|$, we have $\theta_{\mathbf{k}} \to \pi/2$, the s-wave correction vanishes, and the intraband pairings are pure d-wave symmetric, which is actually no surprise due to the proximity effect. However, the interband pairing Δ_{+-} is pure s-wave symmetric, which plays a key role in opening the nodal gap for d-wave pairing.

By diagonalizing the Hamiltonian matrix, we obtain the superconducting quasiparticle spectrum. The quasiparticle dispersion takes the simple form

$$E_{\pm}(\mathbf{k}) = \sqrt{\frac{A_{\mathbf{k}} \pm \sqrt{A_{\mathbf{k}}^2 - 4B_{\mathbf{k}}}}{2}}, \tag{9}$$

where

$$\begin{aligned} A_{\mathbf{k}} &= \epsilon_x^2 + \epsilon_y^2 + 2\epsilon_{xy}^2 + \Delta_{xx}^2 + \Delta_{yy}^2, \\ B_{\mathbf{k}} &= \left(\epsilon_{xy}^2 - \epsilon_x\epsilon_y\right)^2 + 2\Delta_{xx}\Delta_{yy}\epsilon_{xy}^2 + \Delta_{xx}^2\epsilon_y^2 \\ &\quad + \Delta_{xx}^2\Delta_{yy}^2 + \Delta_{yy}^2\epsilon_x^2. \end{aligned} \tag{10}$$

Two quasiparticle bands $E_+(\mathbf{k})$ and $E_-(\mathbf{k})$ are separated, and $E_-(\mathbf{k})$ corresponds to the lower one.

With the expression for the quasiparticle spectra, we are in a good position to examine the gap nodes and the STM probe of the gap. The d-wave pairing in the bulk cuprates has the form of $\Delta_d(\mathbf{k}) \propto (\cos k_x - \cos k_y)$, and there are four nodes along the lines of $k_x = \pm k_y$, which are crossing points of the lines with the Fermi surface. As the intraband pairing is dominated by d-wave pairing form, it is expected that gap nodes in quasiparticle excitations are very likely to occur. However, the mixture with s-wave pairing could potentially open the gap nodes as long as the s-wave component is relatively strong enough, e.g., if t_{xy} is small, and Δ_0 is large. The exact criterion is given by the zeros of $B_{\mathbf{k}}$, which will be discussed in the next section.

III. NODELESS GAP FUNCTION IN TWO-ORBITAL MODEL

In this section, we examine the possibility of a nodeless gap in the two-orbital d-wave superconductivity in the previous section. From Eqs. (9) and (10), the condition for zeros of the quasiparticle is given by $B_{\mathbf{k}} = 0$. This depends on the hopping and pairing parameters. To illustrate the possible nodeless gap, let us first consider a special case: $\epsilon_{xy}(\mathbf{k}) = 0$, namely the interorbital hopping vanishes. In this case, $B_{\mathbf{k}} = 0$ requires both $\epsilon_x(\mathbf{k}) = \epsilon_y(\mathbf{k}) = 0$ and $\Delta_{xx}(\mathbf{k}) = 0$ or $\Delta_{yy}(\mathbf{k}) = 0$. These conditions cannot be satisfied in general except on some discrete parameter space points. This simple example clearly demonstrates the possible nodeless gap in the two-orbital d-wave superconductivity. Actually this corresponds to the limit without hybridization, and the intraband pairing $\Delta_{xx}(\mathbf{k})$ and $\Delta_{yy}(\mathbf{k})$ are effectively C_4 anisotropic extended s-wave pairing. In passing, we note that the d-wave gap function in a two orbital model allows a $\mathbf{k}$-independent term in intraorbital pairing, and the d-wave symmetry only requires the opposite signs of this term for the two different orbitals, as explicitly shown in Eq. (6).

Next, unlike the limit case we demonstrated above, we show that a weak coupling pairing theory does not lead to a gapful d-wave state when $t_{xy} \gg |t_x - t_y|$. This condition is more physically relevant since t_{xy} is the nearest neighbor hopping. Within the weak coupling theory, we may consider only intraband pairing and neglect the interband pairing since the two bands are not degenerate in the presence of the interorbital hopping. Since then the intraband pairing is almost pure d-wave symmetric; the nodal structure in the d-wave pairing therefore remains in two-orbital bands within the weak coupling theory. This shows that the vanishing of the gap nodes requires a strong pairing coupling, comparable to the energy splitting of the two bands. Below we shall consider a representative case to illustrate the gap property. For the monolayer CuO_2, the band structure parameters are not so known, and the proximity-induced pairing strengths are also not known. Therefore the choice of the parameters we will use below is for the purpose of illustration.

We choose a set of parameters $t_{xy} = 1$, $t_x = 0.5$, $t_y = 0.3$ for the noninteracting part of the model. We will discuss the band structure and then examine the gap property. The hybridized bands are plotted in Fig. 2. From Fig. 2, we can see that if $\mu < 0.4$, only the lower hybridized band is partially occupied and the higher band is completely empty. If $0.4 < \mu < 1.6$, we have both the lower band and higher band partially occupied. For further higher chemical potential, $\mu > 1.6$, the lower band is fully occupied. In this paper, we shall focus on the first case. The Fermi surfaces for three typical values of μ within this region are plotted in Fig. 3.

In Fig. 4 we present a "phase diagram" for the nodal d-wave gapless and nodeless d-wave gapful superconducting states in parameter space of Δ_0 and Δ_x and Δ_y. It is interesting to

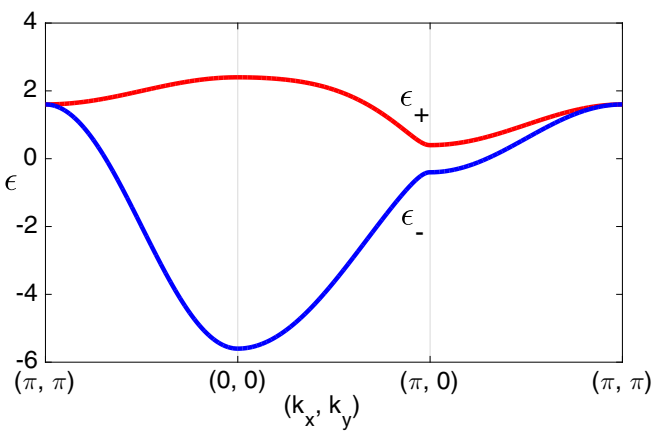

FIG. 2. Two hybridized band dispersions for Hamiltonian H_0 in Eq. (1). The parameters used are $t_{xy} = 1$, $t_x = 0.5$, $t_y = 0.3$. The chemical potential μ is not included or it is set equal to 0.

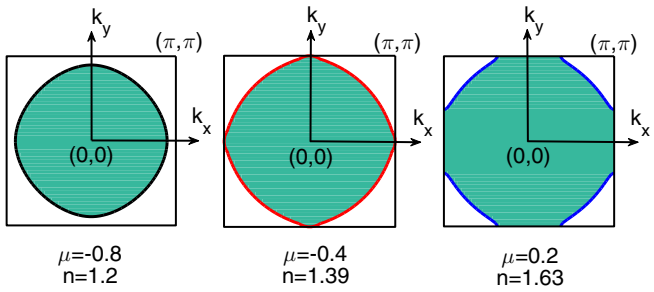

FIG. 3. Fermi surfaces of model Hamiltonian H_0 in the region where the lower energy band in Fig. 2 is partially occupied and the higher energy band is completely empty. The parameters for hopping integrals are the same as in Fig. 2. Three Fermi surfaces correspond to three different values of the chemical potential.

note that the gap property only depends on $\Delta_x + \Delta_y$ instead of each of them in separate forms. At small values of $\Delta's$, the gap has nodes, consistent with the weak coupling pairing analyses. Note that $B_{\mathbf{k}}$ is non-negative, which is required for the quasiparticle solutions as implied in Eq. (9). It can be seen that the nodeless phase only occurs at large values of the on-site pairing strength Δ_0. Qualitatively, we may understand this result as that the gapful phase requires strong interband pairing comparable to the band splitting.

In the nodeless superconducting phase with $\Delta_x = 0.6$, $\Delta_y = 0.3$, $\Delta_0 = 2.1$, and $\mu = 0.2$, the lower quasiparticle band $E_-(\mathbf{k})$ in the Brillouin zone is calculated and displayed in Fig. 5(a). This quasiparticle band has dramatic changes, very different from the corresponding band without the pairing. The local density of states, which is proportional to the local differential tunneling conductance STM probes, can be calculated by using the quasiparticle dispersion and is plotted in Fig. 5(b). Although there appears a U-shaped mini-gap in the lower energy regime, the resonant peak does not reside

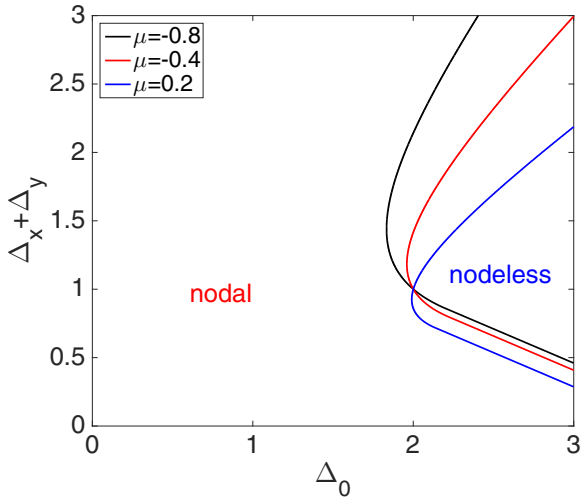

FIG. 4. Phase diagram for the nodal and nodeless gap superconducting states in the proximity-induced two-band superconductivity. Δ_0, Δ_x, and Δ_y are pairing amplitudes defined in Eq. (6). The parameters in the noninteracting two-orbital model H_0 are: $t_{xy} = 1$, $t_x = 0.5$, $t_y = 0.3$, the same as in Fig. 2.

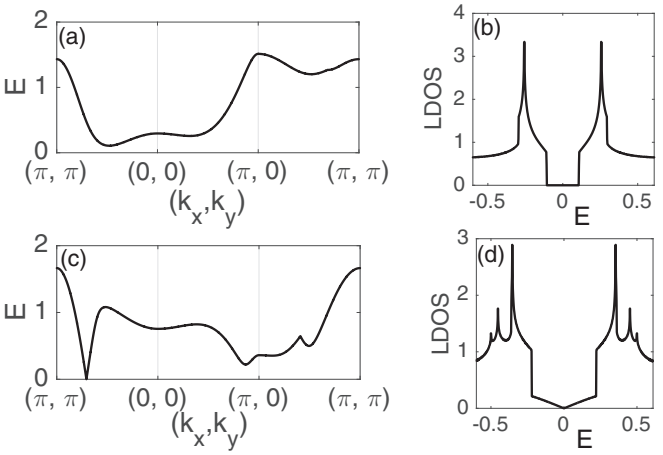

FIG. 5. Upper panel: the lower quasiparticle dispersion $E_-(\mathbf{k})$ (a) and local density of states (b) in the nodeless superconducting phase ($\Delta_0 = 2.1$). Lower panel: the lower quasiparticle band (c) and local density of states (d) in the nodal gap phase ($\Delta_0 = 0.9$). All the other parameters are the same in both phases: $\Delta_x = 0.6$, $\Delta_y = 0.3$, and $\mu = 0.2$, and the noninteracting band structure parameters are $t_{xy} = 1$, $t_x = 0.5$, and $t_y = 0.3$, the same as in Figs. 2–4.

exactly on the edge of the mini-gap, rather different from the conventional single band model, because the resonant peak still originates from d-wave pairing. As a comparison, we also give rise to the results for the nodal superconducting phase with $\Delta_x = 0.6$, $\Delta_y = 0.3$, $\Delta_0 = 0.9$, and $\mu = 0.2$, and the corresponding results are displayed in Figs. 5(c) and 5(d).

In experiment, both the U-shaped and V-shaped energy gaps have been observed on the films at the spatially different regions. We would like to explain that those different regions may have different characteristic parameters, e.g., the pairing amplitudes and doping concentration. So these regions correspond to the nodeless phase and nodal phase of our phase diagram, respectively. Since the actual two oxygen band parameters are not available at present, our aim in this paper is to demonstrate the qualitative feature of the U-shaped STM spectrum from the proximate d-wave superconductivity. More quantitative comparison will be left for future work when the band structure of the oxygen bands and the proximity-induced superconducting order parameters are available.

IV. SUMMARY AND DISCUSSIONS

In summary, the successful growth of the monolayer CuO_2 on Bi-2212 reported by Zhong *et al.* [5] has provided a material, as a complement to bulk cuprates, to study physics in copper oxides. Motivated by their finding, we have proposed that the observed high T_c superconductivity with nodeless gap is proximity-induced superconductivity and that the normal state of the monolayer is described by a two-orbital model. We have further examined the superconducting gap functions in a two-orbital model and demonstrated a mixture of d-wave and s-wave pairing, which may explain the observed U-shaped gap in the experiment. In our calculations, the nodeless gap phase in the two-orbital model occurs in the region where the on-site pairing coupling is strong and comparable to the energy splitting in the two bands.

We wish to point out that the noninteracting two orbital model we used in the paper is a simplified model and the coupling between the O-2p orbitals and the localized spin on the Cu sites has the Kondo type coupling, which is expected to greatly reduce the bandwidths of the O orbitals near the Fermi level. From this point of view, the nodeless gap phase may be realized in the monolayer CuO_2. While our theory is more closely related to the monolayer CuO_2, our results may be relevant to nodeless d-wave superconductivity in heavy fermion superconductor $CeCu_2Si_2$, where the superconductivity is believed to have d-wave symmetry [12], but recent specific heat data and superfluid density indicates a full gap in its low-energy excitations [13,14].

After finishing this paper, we noticed that nodeless excitation spectrum in a two-orbital model with d-wave symmetry was previously discussed in the context of iron based superconductivity [15]. In that case, the reason for gapful excitations is due to the lack of intersection of the Fermi surfaces and the line nodes of the superconducting gap function, similar to the limiting case with vanishing interorbital hopping term we discussed in the beginning of the third section in this paper. In contrast, a more physically relevant case we discussed in this paper as illustrated in Figs. 2–5 has a large interorbital hopping integral, and the gapful excitation results from the large interband pairing.

ACKNOWLEDGMENTS

We thank Qi-Kun Xue and his group members for stimulating discussions on their experiments. We also thank W. Q. Chen for helpful discussions, especially on the proximity-induced pairing strength including the on-site pairing. G.M.Z. acknowledges the support of NSF-China through Grant No. 20121302227, and F.C.Z. is supported in part by National Basic Research Program of China (under Grant No. 2014CB921203) and NSFC (under Grant No. 11274269).

[1] J. G. Bednorz and K. A. Müller, Z. Phys. B **64**, 189 (1986).
[2] P. W. Anderson, Science **235**, 1196 (1987).
[3] P. W. Anderson, P. A. Lee, M. Randeria, T. M. Rice, N. Trivedi, and F. C. Zhang, J. Phys. Condens. Matter **16**, R755 (2004).
[4] P. A. Lee, N. Nagaosa, and X. G. Wen, Rev. Mod. Phys. **78**, 17 (2006).
[5] Y. Zhong, Y. Wang, S. Han, Y.-F. Lv, W.-L. Wang, D. Zhang, H. Ding, Yi.-M. Zhang, L. L. Wang, K. He, R. D. Zhong, J. A. Schneeloch, G.-D. Gu, C.-L. Song, X.-C. Ma, and Q.-K. Xue, Sci. Bull. **61**, 1239 (2016).
[6] F. C. Zhang, Sci. Bull. **61**, 1236 (2016).
[7] Z.-X. Shen, D. S. Dessau, B. O. Wells, D. M. King, W. E. Spicer, A. J. Arko, D. Marshall, L. W. Lombardo, A. Kapitulnik, P. Dickinson, S. Doniach, J. DiCarlo, T. Loeser, and C. H. Park, Phys. Rev. Lett. **70**, 1553 (1993).
[8] D. A. Wollman, D. J. Van Harlingen, W. C. Lee, D. M. Ginsberg, and A. J. Leggett, Phys. Rev. Lett. **71**, 2134 (1993).
[9] C. C. Tsuei, J. R. Kirtley, C. C. Chi, Lock See Yu-Jahnes, A. Gupta, T. Shaw, J. Z. Sun, and M. B. Ketchen, Phys. Rev. Lett. **73**, 593 (1994).
[10] F. C. Zhang and T. M. Rice, Phys. Rev. B **37**, 3759 (1988).
[11] W. Q. Chen, private communications (2016).
[12] F. Steglich, J. Aarts, C. D. Bredl, W. Lieke, D. Meschede, W. Franz, and H. Schafer, Phys. Rev. Lett. **43**, 1892 (1979).
[13] S. Kittaka, Y. Aoki, Y. Shimura, T. Sakakibara, S. Seiro, C. Geibel, F. Steglich, H. Ikeda, and K. Machida, Phys. Rev. Lett. **112**, 067002 (2014).
[14] G. M. Pang, M. Smidman, J. L. Zhang, L. Jiao, Z. F. Weng, E. M. Nica, Y. Chen, W. B. Jiang, Y. J. Zhang, H. S. Jeevan, P. Gegenwart, F. Steglich, Q. Si, and H. Q. Yuan, arXiv:1605.04786.
[15] E. M. Nica, R. Yu, and Q. Si, arXiv:1505.04170.